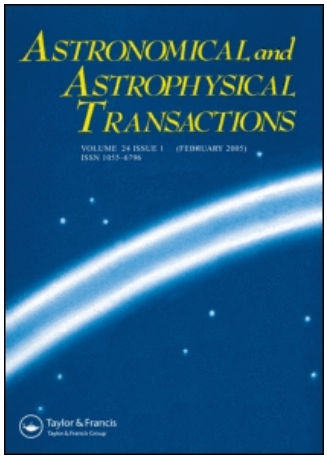

Astronomical & Astrophysical Transactions
The Journal of the Eurasian Astronomical Society
Publication details, including instructions for authors and subscription information:
http://www.informaworld.com/smpp/title~content=t713453505

Temperature and density in the middle corona through the activity cycle determined from white light observations

O. G. Badalyan

Online Publication Date: 01 March 1996
To cite this Article: Badalyan, O. G. (1996) 'Temperature and density in the middle corona through the activity cycle determined from white light observations', Astronomical & Astrophysical Transactions, 9:3, 205 - 223
To link to this article: DOI: 10.1080/10556799608208224
URL: http://dx.doi.org/10.1080/10556799608208224

Astronomical and Astrophysical Transactions, 1995, Vol. 9, pp. 205–223
Reprints available directly from the publisher
Photocopying permitted by license only

TEMPERATURE AND DENSITY IN THE MIDDLE CORONA THROUGH THE ACTIVITY CYCLE DETERMINED FROM WHITE LIGHT OBSERVATIONS

O. G. BADALYAN

IZMIRAN, Troitsk, Moscow Region, 142092, Russia

(Received March 15, 1995)

We investigated the solar cycle variations of the physical characteristics of coronal plasmas in equatorial regions and polar holes in the range from 1.2 to $2.5R_\odot$ from the Sun's center. We use coronal white light data obtained from total solar eclipses since the 1950s. To eliminate the effects of inhomogeneous data, all observational results for each eclipse were reduced to a common system in which the F-corona model of Koutchmy and Lamy (1985) was used as the photometric standard. Then the K-coronal brightness was determined by subtracting the F corona brightness from the total $K+F$ emission. Values of temperature and density were determined by comparing the observed brightness distributions with distributions calculated assuming a hydrostatic and isothermal corona. We find that in equatorial regions the temperature in the middle corona is constant and equal to 1.4×10^6 K, but n_0, the parameter of the hydrostatic distribution, gradually increases from 2×10^8 cm^{-3} at solar minimum to 4×10^8 cm^{-3} at maximum. The specific value of n_0 depends on the level of activity of the underlying solar regions and could be connected with the presence of coronal streamers. In polar regions, n_0 does not depend on the phase of the cycle and is apparently determined by the properties of the associated hole; those values vary in the range from 0.65 to 1.4×10^8 cm^{-3}. The temperature in polar regions increases from 0.9×10^6 K at minimum to 1.4×10^6 K at maximum. Above $2.5R_\odot$, a deviation from the hydrostatic density distribution is found, which is most likely connected with the gas-dynamical coronal expansion developing at these heights. The emission measure and mass of the entire corona are evaluated.

KEY WORDS Solar corona, physical conditions, activity cycle

1 INTRODUCTION

In the past 25 years significant progress has been attained in EUV and X-ray observations of the solar corona. They have permitted important advances in our understanding of the inner corona; the structure, the physical conditions and their variations with phase of the cycle, as well as rapid and eruptive dynamical phenomena have been studied. However, for the more distant regions of the middle and outer corona the primary source of information is still optical observations.

The basic structural elements of the inner quiet corona are loops of various sizes. The 11-year activity cycle of the inner corona is very clearly evident in the variation of the total emission measure of these loops. Variations are observed in the soft X-ray emission as well as in the coronal green line (5303 A) emission from those regions. These variations are due primarily to changes in the total number of loops, which appear mostly, of course, in the coronal equatorial regions.

The middle and outer corona also reveal cyclic variations. These are the well known variations of the general coronal form (i.e., the flattening) and of the structural details, e.g., the increase of the number of coronal rays at maximum activity and growth of polar coronal hole areas at minimum. The variations of the physical parameters, i. e., the temperatures and densities, have not been well studied in these regions. Two classical papers are basic in this area. The first is the paper by Van de Hulst (1950), in which he constructed a spherically-symmetric model of the K-corona for the period of maximum activity and a model with different density functions for the equatorial and polar regions at minimum. The second one is the work by Saito (1970) in which all brightness and polarization measurements of the white-light corona obtained by that time were summarized and analyzed, and an axially symmetric model of the K-corona was constructed for solar minimum.

The goal of this paper is the study of the cyclical variations of temperature and density, generally in the middle corona at distances from 1.2 to 2–2.5$R_\odot$ from the Sun's center. We examine equatorial regions of the corona and regions of high-latitude coronal holes (more precisely, the regions of lowest brightness in eclipse white-light photographs). We also devote some attention to the equatorial outer corona in regions above 2.5$R_\odot$. The best data for this work appear to be the white-light coronal data obtained during total eclipses through several activity cycles.

Although there is a large number of white-light coronal observations, the nonuniformity of the data make their statistical treatment difficult. This is due to many factors: the very limited times of observation, and in addition, in field conditions, difficulties in photographing a faint object and in carrying out absolute measurements (i.e., comparisons with the brightness of the center of the solar disk), and to other reasons well known to all observers. Therefore, to obtain temperatures and densities characterising each eclipse, a method was developed to reduce all observations to a common system. In this procedure, the following two factors are of importance:

1) In preceding work (Badalyan and Livshits, 1985, 1986a; Badalyan, 1986a) we presented and developed a new method for the analysis of white-light coronal data, in other words, a new method for dealing with an ill-posed problem, namely, the solution of an integral equation. In this method we assume a priori a model of the distribution of temperature and density in the corona. The distribution of the brightness of the K-corona, B_K, as a function of distance from the Sun's center, ρ, is computed and compared to the observations. This comparison, carried out in our paper cited above, showed that in the middle corona the dependence of $B_K(\rho)$ agreed with the model of hydrostatic density distribution with T =const. This result followed with surprising consistency from the comparisons of the observed and theoretical distributions for all large-scale structures and for all eclipses. It

therefore proved possible to use the method to reduce data from various authors to a common system and to determine more precisely the temperature T and density n_0, the parameters of the hydrostatic distribution.

2) To obtain absolute values of corona brightness, that is, to obtain the values of n_0 corresponding to various eclipses on one brightness scale, the F-corona model of Koutchmy and Lamy (1985) is used as a photometric standard. This is one of the most recent models; the authors analyzed all previous models of the F-corona, and at present it is the best model. We further note that the use of any other model of the F-corona leads only to a general displacement of the entire density scale, but does not change the essential results of our work.

We now consider these two points in more detail.

2 THE METHOD OF DETERMINING TEMPERATURE AND DENSITY IN THE MIDDLE CORONA

The basic observed quantity which is used to find the temperature and density of the plasma in the middle and outer corona is the surface brightness B as a function of the distance from the Sun's center, ρ. The widely known method of determining density was introduced by Baumbach (1937); at the present time this generally accepted standard method of analyzing white-light coronal data. In this method, the observed brightness $B(\rho)$ is represented as a sum of a series of terms C_m/ρ^m, where C_m are constants and $m > 0$, and then the Abel equation is solved. This method and its modifications have been employed repeatedly and continue to be used today. A number of authors, beginning with Van de Hulst (1950), found hydrostatic distributions of density below $2.5R_\odot$. In Badalyan and Livshits (1985, 1986a) and Badalyan (1986a) we showed how this fact gives rise to the universal form of the observed $B_K(\rho)$, appearing particularly clearly in the dependence of $\ln B_K$ on $R_\odot/\rho$.

Therefore in the method we introduced for the theoretical calculation of B_K we took the model of the hydrostatic distribution of density with T =const:

$$n(r) = n_0 \exp(-b/R_\odot) \exp(b/r), \tag{1}$$

where

$$b = \mu m_H g_\odot R_\odot^2/(kT). \tag{2}$$

Here we use standard symbols, r is the heliocentric distance of the emitting point along the line of sight, and $\mu \approx 0.6$.

For isotropic Thomson scattering, Badalyan and Livshits (1985) (see also Badalyan and Livshits, 1986a) derived an analytical expression for $B_K(\rho)$ for a hydrostatic density distribution with T =const.

For an anisotropic scattering coefficient, the intensity and polarization of the K corona were numerically obtained by Badalyan (1986a) by calculating $K_t \pm K_r$, the tangentially and radially polarized components respectively, of the radiation. In the present study we consider the theoretical dependence of $K_t + K_r$ on $R_\odot/\rho$.

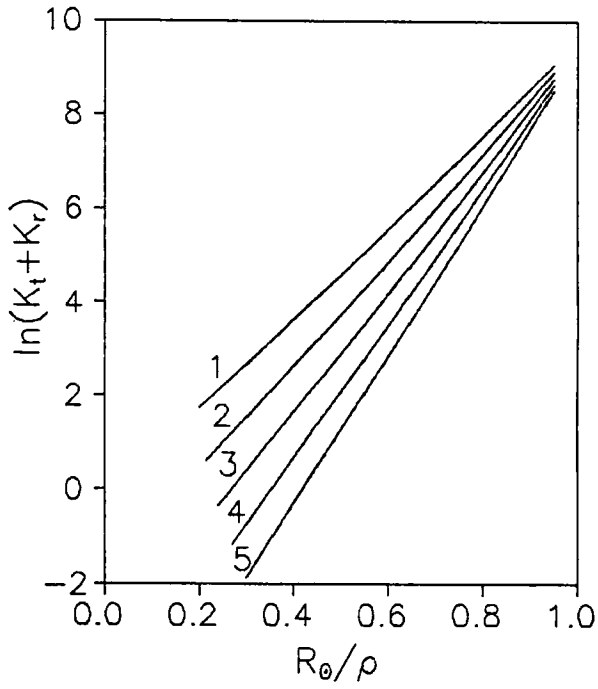

Figure 1 Theoretical brightness distributions of the K-corona for $n_0 = 10^8$ cm^{-3} and a range of temperatures: 1, 1.62; 2, 1.38; 3, 1.20; 4, 1.06; 5, 0.95 x 10^6 K.

In Figure 1 are shown a family of curves of $\ln(K_t + K_r)$ for values of b ranging from 8.5 to 14.5 in steps of 1.5. These curves were calculated for the case of the no limb darkening ($q = 0$). As was shown by Badalyan (1986a), the influence of q is significant only in the lowest part of the corona at $\rho < 1.15R_\odot$, and is therefore not examined in the present study. The parameter n_0 is assumed to be 10^8 cm^{-3} for the calculations.

The method of determining the temperature T and density n_0 consists of the following. We calculate a family of theoretical curves for a set of temperatures and a fixed value of n_0. In the plot of $\ln(K_t + K_r)$ against $R_\odot/\rho$ (Figure 1), the assumed temperature determines the slope of the theoretical curve. As seen in Figure 1, the dependence of the functions $\ln(K_t + K_r)$ on $R_\odot/\rho$ is practically linear. To determine the density, we note that the value of n_0 enters the expression for $K_t \pm K_r$ as a factor (see Badalyan, 1986a). Therefore a change of the parameter of the hydrostatic distribution leads to a shift of the family of curves as a whole along the ordinate. Thus, the determined values of the logarithms of the K-coronal brightness, $\ln B_K$, are plotted as functions of $R_\odot/\rho$ and then superposed on the family of theoretical curves. The theoretical curve whose slope gives the best fit to the observational data yields the value of the temperature, while the shift along the ordinate allows us to determine n_0.

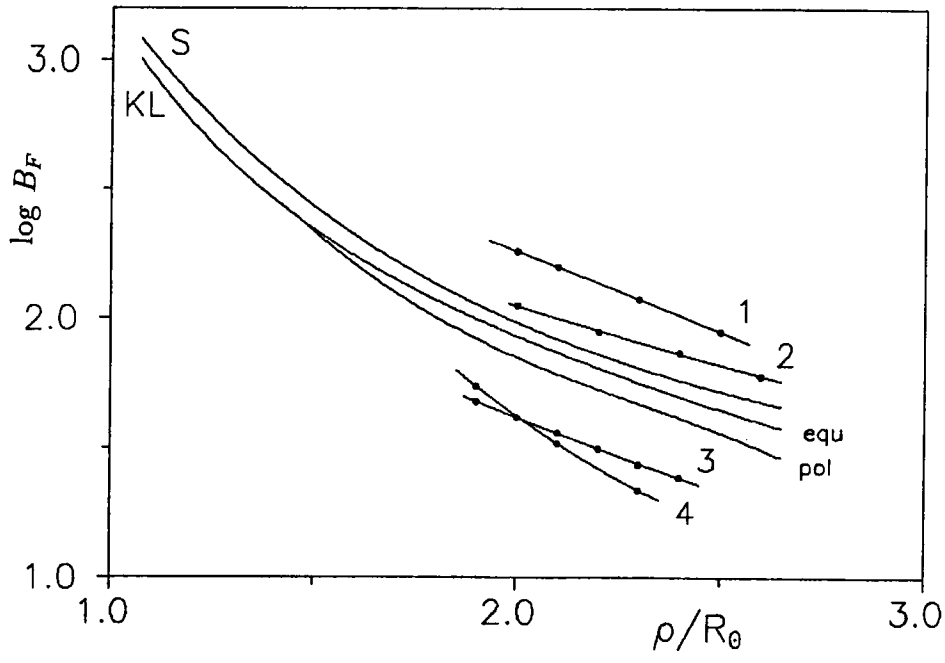

Figure 2 F-corona models: S, Saito (1970); KL, Koutchmy and Lamy (1985); $K + F$ coronal brightness at the pole for several observations: 1, Saito and Hata (1970); 2, Waldmeier (1964); 3, Waldmeier (1966); 4, Rušin and Rybanský (1976).

3 USE OF THE MODEL F-CORONA AS AN ABSOLUTE STANDARD OF BRIGHTNESS

We see that, to isolate the K-corona independently of an assumed F-corona model, it appears best to use the polarized brightness values, pB, i.e., data either from polarization eclipse observations or from K-coronameters. It is clear, however, that for our purpose there are not enough such data. In addition, the significantly increased difficulties in making polarization measurements result in loss of measurement accuracy.

The F-corona model was earlier used as a standard for determining absolute intensities for example by Koutchmy and Magnant (1973). Badalyan (1986a) presented a method for obtaining the absolute values of polarized brightness, pB, for the case when the eclipse relative brightness and the degree of coronal polarization had been obtained.

In this paper the assumed F-corona model of Koutchmy and Lamy (1985) is used to reduce all eclipse white-light coronal data to a single system, after which the F-corona is subtracted from the total $K + F$ intensity to determine densities n_0 on a single scale.

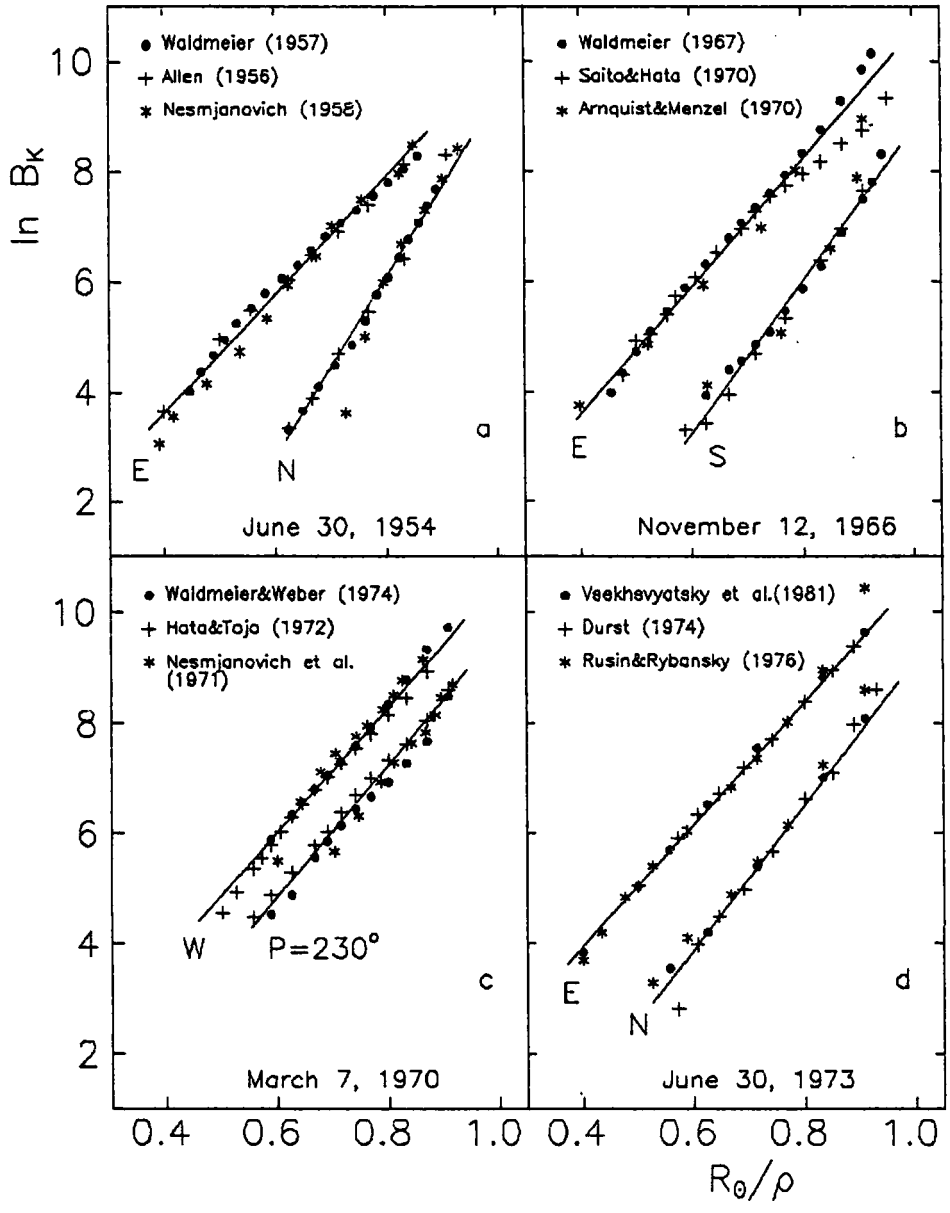

Figure 3 *K*-corona brightness for several eclipses and theoretical fits to the data.

Models of the F corona of Saito (1970) and of Koutchmy and Lamy (1985) are shown in Figure 2. While the model of Saito (1970) is spherically symmetric, that of Koutchmy and Lamy (1985) is more general, so that their F-corona intensities, B_F, differ in the polar and equatorial directions above $1.5R_\odot$.

It is well known (Van de Hulst, 1950) that during solar minimum the F-corona becomes dominant at low heights in the polar regions. At a height of $2R_\odot$ the K-corona has already fallen to only 10% of the total brightness. We can generally assume that the polar coronal emission measured above that height is due almost completely to the F corona. This is the basis for our use of the F-corona model as the absolute standard of photometric brightness.

As seen in Figure 2, the F corona of Koutchmy and Lamy (1985) is fainter than that of Saito (1970); the average difference in log B_F is about 0.1. Since the $K+F$ brightness scales with the assumed F-corona brightness, the K-corona brightness and corresponding density will be a factor of 1.26 lower for the Koutchmy and Lamy (1985) model than for the Saito model (1970).

The basic difficulty in subtracting the F-corona from total coronal emission is due to the errors in the absolute values of the brightness obtained from the eclipse photographs. This is illustrated in Figure 2 where we plot values of the total brightness of the $K+F$ corona obtained during several eclipses. Data of different authors for the same eclipses deviate from the assumed standard F-coronal model in various ways (see also Table 1). This scatter of absolute brightness values further reflects the serious difficulties with which coronal observes are confronted during eclipses.

Thus, from a comparison of the observed brightness in the faintest polar region of the corona with an assumed F-corona model at distances $\rho > R_\odot$ we determine the value $\Delta = \log B_F - \log B$ (these values are given in Table 1). All values of brightness, obtained by a given author for a specific eclipse, are corrected by the corresponding values of Δ, and then F-corona is subtracted. Logarithms of the K-coronal brightness B_K determined by this procedure are plotted as functions of $R_\odot/\rho$. Data of different authors pertaining to a single eclipse are plotted on each graph of Figure 3, from which the quantities T and n_0 are determined as described above.

In practice, since data of various authors differ not only by errors in absolute measurements but also by various other photometric errors, it frequently happens that even when we achieve good agreement in the brightness of the polar regions, a large scatter of equatorial region data results. Therefore we must use several iterations in the values of Δ to minimize the dispersion of ln B_K at different positional angles.

In this method it is possible to use coronal brightness measurements in arbitrary units since their comparison with the standard F-corona model results in a reduction to absolute values of B_K.

Investigations of coronal brightness at solar maximum are especially difficult. At such times the corona is almost spherically symmetric, and even at $4R_\odot$ the K corona contributes substantially to the total emission. For a particular eclipse at maximum, only the absolute brightness measurements can be used directly. After those values are averaged, one can add the measurements of the other observers given in arbitrary units by finding a best fit to the average derived from absolute values. One can constrain these derived of B_K using the height dependence of the relative K-coronal contribution to the total coronal brightness at maximum introduced by Van de Hulst (1950).

Table 1. Eclipses Analyzed in the Study*

Date	φ_1 *from (3),(4)*	φ_2 *from (5)*	*Refernces, annotation*	*units*	$\Delta = log B_F - log B$
25.02.52	−0.34	0.77	Von Kluber (1958), Figs. 5 and 6	abs	−0.15
			Hepburn (1955), Figs. 4a, b	"	+0.1
			Mikhel'son (1955), Table 5, direct. XIII, IX	arb	
			Nikolsky (1954), Figs. 2 and 3.	"	
			Dürst (1973), Tabl. 7b.	abs	−0.1
30.06.54	0.00	0.00	Waldmeier (1957), Tabl. 4	abs	−0.05
			Allen (1956), Tabl. 2	"	−0.1
			Nesmjanovich (1958), Fig. 1	arb	
20.06.55	+0.28	0.09	Saito (1956), Tabl. 3	abs	−0.05
			Waldmeier *et al.* (1957), Table.8	arb	
12.10.58	−0.87	0.42	Waldmeier (1959), Tabl. 1	arb	
			Saito and Yamashita (1962), Tabl. 2	abs	−0.2
15.02.61	−0.53	0.64	Waldmeier (1962), Tabl. 4	abs	+0.4
			Löchel and Högner (1965), Tabl. 2	"	+0.35
			Leksa (1963), Fig. 3	arb	
5.02.62	−0.39	0.74	Waldmeier (1963), Tabl. 4	abs	−0.1
			Owaki and Saito (1967), Tabl. 2	"	−0.15
20.07.63	−0.18	0.88	Waldmeier (1964), Tabl. 3	abs	−0.1
			Gillett *et al.* (1964), Fig. 3	"	−0.45
30.05.65	+0.15	0.05	Waldmeier (1966), Tabl. 5	abs	+0.25
12.11.66	+0.50	0.18	Waldmeier (1967), Tabl. 5	abs	+0.1
			Saito and Hata (1970), Tabl. 5	"	−0.35
			Arnquist and Menzel (1979), Fig. 2	arb	

22.09.68	+0.96	0.34	Waldmeier and Weber (1969), Tabl. 2	abs	
			Khetsuriani *et al.* (1971), Tabs. 5 and 6	"	
			Nesmjanovich *et al.* (1971a), Fig. 1	arb	
7.03.70	−0.83	0.46	Waldmeier and Weber (1974), Tabs. 5 and 6	abs	−0.1
			Hata and Tojo (1972), Tabl. 4	"	−0.15
			Nesmjanovich *et al.* (1971b), Fig. 1	"	+0.15
10.07.72	−0.52	0.66	Koutchmy *et al.* (1974), Fig. 3	abs	−0.2
			Koutchmy *et al.* (1975), Fig. 3	arb	
			Nesmjanovich and Popov (1976), Fig. 2	"	
30.06.73	−0.39	0.74	Vsekhsvyatsky et al. (1981), Fig. 6	abs	+0.05
			Dürst (1974), Tabs. 5 and 6	"	−0.2
			Rušin and Rybanský (1976), Tabl. 1	"	+0.3
23.10.76	+0.09	0.03	Dürst (1979), Tabl. 7	abs	0.0
16.02.80	−0.97	0.35	Dürst (1979), Fig. 8	abs	
			Street and Lacey (1982), page 83	"	
			Rušin and Rybanský (1983), Tabl. 4	"	
			Badalyan *et al.* (1993), Fig. 2	arb	
11.06.83	−0.45	0.69	Koutchmy and Nitschelm (1984), Fig. 3	abs	0.0

Note. *List of eclipses; phase φ_1 from (3) and (4) and φ_2 from (5), references and notes about the data; $\Delta = \log B_F - \log B$ is the difference between the assumed model of the F-corona and the data in cases when measurements were carried out in absolute units (B_F and B in units of $10^{-10}\overline{B}_\odot$). Δ was not determined for eclipses during the solar maxima years of 1968 and 1980.

4 OBSERVATIONAL MATERIAL

Extensive observational material obtained during total eclipses is presently available. In the analysis of this material it was necessary to exercise some minimal selection of the data.

For the following analysis, a number of eclipses were selected which occurred since the 1950s. Among them, the study by M. Waldmeier is prominent. These are the best observations, carried out uniformly and including nearly all eclipses of the period we examine. His work, with rare exceptions, was excellent in terms of both relative and absolute measurements, and the results themselves can be considered to be standards. We note with regret that current photometric work is carried out with far less care, in spite of more advanced technology.

The list of eclipses we use presented in Table 1, where we also give brief notes concerning the results derived from the observations. In the table we also show the phases of the activity cycle, determined by two methods. The first one was introduced by Ludendorf: the phase φ_1 of the time t is given by:

$$\varphi_1 = (t - m)/(m - M_1), \quad \text{if } M_1 < t < m \tag{3}$$

$$\varphi_1 = (t - m)/(m - M_2), \quad \text{if } m < t < M_2 \tag{4}$$

where M_1 and M_2 are the times of two successive maxima and m the time of the minimum between M_1 and M_2. With this definition, the duration of the shorter rise phase is somewhat extended, and that of the decline is shortened.

Another definition of the phase was frequently used by Waldmeier (e.g., Waldmeier, 1957) in studies of the variation of the general coronal flattening with time:

$$\varphi_2 = (t - m_1)/(m_2 - m_1) \tag{5}$$

where m_1 and m_2 are the times of two consecutive minima. The point of maximum for this definition occurs when $\varphi_2 = 0.35$. The asymmetry of the rise and decay phases of the activity cycle is well represented in this definition.

The times of solar maximum and minimum are taken from Table 18 of Vitinsky *et al.* (1986) and from Solar-Geophysical Data for the 22nd cycle.

5 SUMMARY OF RESULTS

The determination of n_0 and T was carried out for both the east and west equatorial regions and for the faintest polar directions identified with coronal holes. Examples of such plots are shown in Figure 3 (a–d) for several eclipses. In each of these figures, data from one equatorial limb and a polar direction are presented (for the eclipse of 1970, the hole position angle was $P = 230°$). Straight lines show the theoretical values of $\ln(K_t + K_r)$ which best fit the observations. As seen in Figure 3, the polar plots usually have the larger slopes, due to the lower temperatures in holes.

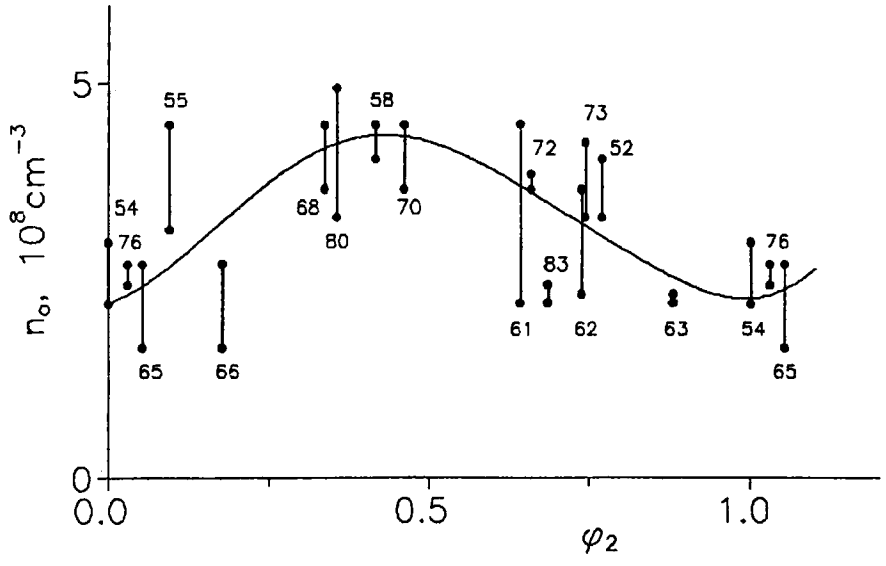

Figure 4 Densities n_0 of equatorial regions as a function of the phase of the activity cycle determined from (5).

The data of different authors agree well in some cases, but in other cases there are significant differences due to observational errors.

The resulting values of the temperatures T and densities n_0 are compiled in Table 2. The values of $\Delta = \log B_F - \log B$, i.e., the difference between the values of brightness obtained by each author for large distances in the polar direction (essentially, the F-corona of a given author) and the assumed F-corona model of Koutchmy and Lamy (1985), were given earlier in Table 1. The average of all the delta values in Table 1 is 0, in our opinion, due to this excellent model of the F corona.

In Figure 4 we plot the equatorial values of n_0 as a function of the solar cycle phase φ_2 calculated from equation (5). Values derived for the west and east limbs are linked with vertical lines. From Figure 4 we see that at minimum phase $n_0 \approx 2 \times 10^8$ cm^{-3}, then it increases at maximum, reaching $\approx 4.3 \times 10^8$ cm^{-3} (for the F corona model of Saito 1970 the latter value would be 5.4×10^8 cm^{-3}). These values agree with previous results, for example, by Van de Hulst (1950). It can also be seen in Figure 4 that the density increase from minimum to maximum and its subsequent drop reflect the asymmetric rise and fall of solar activity. Values of density at each limb depend on the activity level of the underlying solar region. Sometimes the east and west limbs differ significantly (e.g., for the eclipse of 15 February 1961), and sometimes they practically coincide (e.g., for the eclipses of 20 July 1963 and 10 July 1972).

As indicated in Table 2, the temperature of the equatorial regions of the middle corona is practically constant and equal to 1.4×10^6 K. This is apparently related

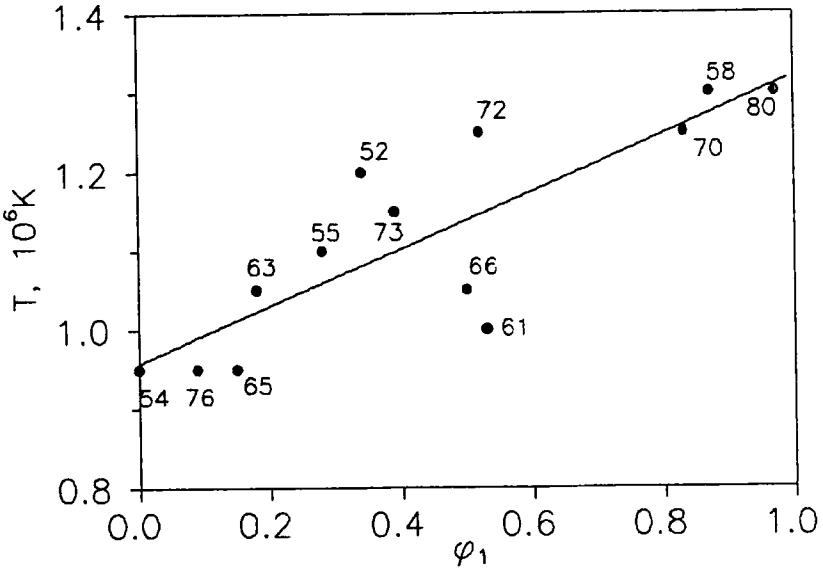

Figure 5 Temperatures in coronal holes (polar regions). Phase of the cycle determined from (3) and (4).

to the general energy balance in the equatorial regions of the middle corona at 1.2–$2.5R_\odot$.

Now we turn to the physical characteristics of the regions identified with coronal holes. As seen from Table 2, no apparent dependence of hole densities on the phase of the cycle is observed. The value of n_0 is determined by the properties of each particular hole, possibly by its size. At solar minimum the coronal hole densities range from 0.65×10^8 to 1.4×10^8 cm^{-3}. At solar maximum the polar regions are only nominally identified with coronal holes.

The temperature variation in coronal holes through the activity cycle is more interesting. In Figure 5 we plot temperatures in holes as a function of the cycle phase φ_1 from equations (3) and (4). In view of the paucity of data, no distinction between positive and negative values of φ_1 is made. From Figure 5 we see that, at solar minimum, holes have a temperature of about 0.9×10^6 K; it increases toward maximum and becomes equal to that of equatorial regions.

6 THE OUTER CORONA. THE EFFECT OF THE GASDYNAMIC EXPANSION OF THE CORONA

The gravitational force weakens with distance from the Sun, but the plasma temperature does not significantly change. As a result, at some distance, gravity no longer restrains the hot plasma, which begins to flow outward. Therefore, the white-light

Table 2. Summary of temperatures T and densities n_0 in equatorial regions and in coronal holes (polar regions)

Data of eclipse	*E-limb*		*W-limb*		*Coronal hole (polar region)*		
	n_0, 10^8 cm^{-3}	T, 10^6 K	n_0	T	P	n_0	T
25.02.52	4.1	1.3	3.3	1.4	N	1.4	1.2
30.06.54	2.2	1.4	3.0	1.4	N	1.0	0.95
20.06.55	4.5	1.3	3.2	1.35	S	1.65	1.1
12.10.58	4.5	1.4	4.0	1.4	S	2.1	1.3
15.02.61	4.5	1.4	2.2	1.35	N	0.9	1.0
5.02.62	2.3	1.4	3.7	1.4	S	0.9	1.2
20.07.63	2.2	1.4	2.3	1.4	N	1.1	1.05
30.05.65	2.7	1.4	1.65	1.4	S	1.0	0.95
12.11.66	2.7	1.4	1.65	1.3	S	0.65	1.05
22.09.68	4.5	1.4	3.7	1.4	S	1.65	1.4
7.03.70	4.5	1.5	3.7	1.4	230°	1.4	1.25
10.07.72	3.7	1.4	4.5	1.4	N	0.65	1.25
30.06.73	3.3	1.4	4.1	1.4	N	0.9	1.15
23.10.76	2.7	1.4	2.5	1.35	N	1.2	0.95
16.02.80	4.9	1.4	3.3	1.4	S	2.5	1.3
11.06.83	2.2	1.35	2.5	1.35			

observations could be a source of some information about the properties of the solar wind in regions near the Sun.

The effect of coronal expansion on the density distribution (and, consequently, on the brightness) was considered in detail by Badalyan (1988). this effect results in a departure of the observed brightness B_K or of the polarized brightness pB from the theoretical curve calculated at $\rho > 2.5R_\odot$ for assumed hydrostatic equilibrium. Hence, at these distances a different theoretical model is needed, and a coronal model with gasdynamic expansion was considered in Badalyan (1988). The calculations were done for a spherically-symmetric corona with $T = 1.4 \times 10^6$ K. Below $2R_\odot$ a hydrostatic density distribution was assumed, but above $2R_\odot$ the plasma outflow is described by the Parker solution for an isothermal corona. The comparison between the theoretical distribution and observations has shown that the general form of the calculated curve corresponds to the observed behavior of pB in Saito's (1970) empirical model. The flow becomes supersonic at $5R_\odot$.

The method developed by Badalyan (1988) can be applied to large coronal holes having no distinct structure. The large coronal hole of 1973 was examined by Badalyan and Livshits (1986b). Polarization brightness below $2R_\odot$ was taken from eclipse data of Koutchmy (1977), and noneclipse observations obtained on Skylab allowed us to extend the analysis to $5R_\odot$. We found that the variation with height of the polarization brightness in the coronal hole is similar to that of the quiet corona, i.e., below $2R_\odot$ the density distribution is close to hydrostatic one, but above that level it agrees with the Parker model of plasma flow. However, the effect of high-speed streams on the white-light corona is not apparent at these distances.

The effect of plasma flows on the brightness of nonspherically-symmetric structures, namely, coronal streamers, was examined in Badalyan and Livshits (1989). As shown by Dolfus and Mouradian (1981) and by us (Badalyan and Livshits, 1989), the density distribution in streamers is close to hydrostatic out to large distances. There is, however, some deviations of the observations from the theoretical curve calculated for a cylinder with hydrostatic distribution of density for $\rho > 5R_\odot$. Therefore, Badalyan and Livshits (1989) considered a modified model of a Parker flow in a slowly diverging structure (see Badalyan, 1992). It was found that the observations correspond to the model with the critical point at $7.6R_\odot$. In this model, the speed at $25R_\odot$ equals 300 km/s, corresponding to a low-speed solar wind.

From the eclipse data we selected, four eclipses of Dürst in which accurate measurements were made in absolute values of brightness to great distances. These are the eclipses of 1952, 1973, 1976, and 1980. The data were corrected with the values of Δ given in Table 1. The K-coronal brightness values obtained out to $5R_\odot$ are shown in Figure 6. The theoretical curves of $\ln(K_t + K_r)$ were calculated for hydrostatic density (1) and for a corona with gasdynamic expansion (2). For the calculations, the temperature was assumed to be 1.4×10^6 K. Both curves of Figure 6 were calculated for a hydrostatic density parameter $n_0 = 10^8$ cm^{-3}. The observed values of B_K are shifted downward along the ordinate by amounts corresponding to the values n_0 listed in Table 2 (for example, for the 1952 eclipse, this shift amounts to 1.2 in ln B_K, corresponding to the density 3.3×10^8 cm^{-3}).

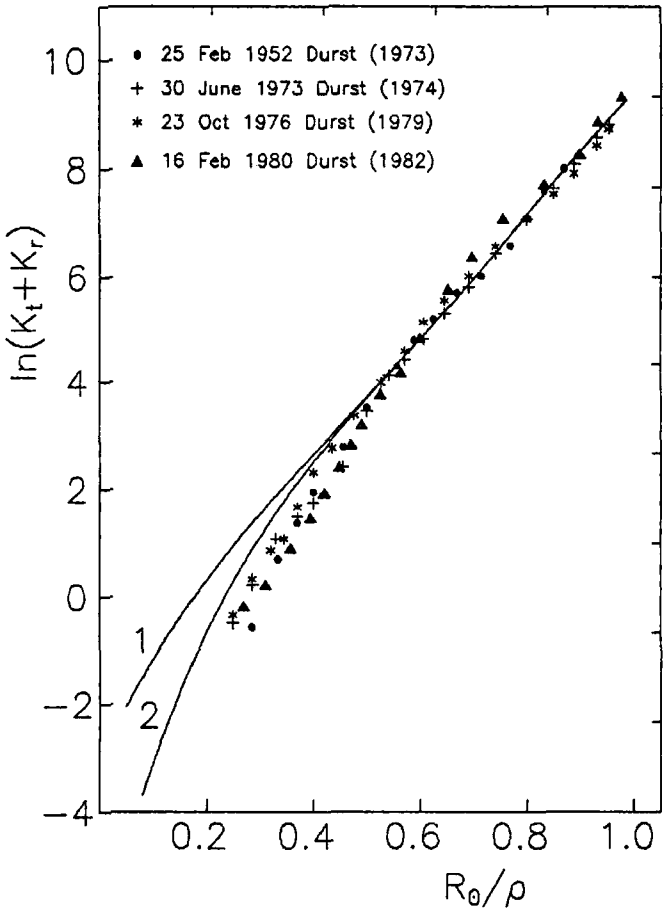

Figure 6 Brightness distribution in the middle and outer corona from four eclipses. Theoretical curves calculated assuming: 1, hydrostatic density distribution; 2, hydrodynamic expansion of an isothermal corona above $2R_\odot$.

As seen in Figure 6, despite the obvious difficulty of observing the corona at large distances, the derived values of brightness certainly show the peculiar property described above: all four distributions deviate from the theoretical hydrostatic curve (1) and lie rather close to the curve (2) calculated for the model of coronal gasdynamic expansion.

In conclusion, we note that in principle the observed departure of the observations from the spherically-symmetric hydrostatic model could also be due to the inhomogeneity of coronal structure above $2R_\odot$. Let us assume that the entire corona consists of dense, radial cylindrical rays. Then the relative contribution of emission from these dense structures to the total brightness (integrated along the line of sight) will decrease with distance from the limb. The density distribution in each of the rays is close to hydrostatic one, since for plasma flow in a cylinder the critical

point is located at infinity. In that case the dependence of brightness on distance will be close to the curve (2) in Figure 6, that is, it will deviate below the brightness curve of the hydrostatic model. A realistic model would probably be a combination of these two possibilities.

7 TOTAL EMISSION MEASURE AND MASS OF THE SOLAR CORONA

The coronal emission measure characterizes the radiative power of the entire corona and its variation with solar cycle. Badalyan (1986b) derived and applied an analytical expression for the coronal emission measure as a function of the temperature and density n_0. Using Figure 1 of Badalyan (1986b) and the value $n_0 = 4.3 \times 10^8$ cm^{-3} found in Figure 4 at solar maximum, we calculate $EM = 5 \times 10^{49}$ cm^{-3}. For the corona at minimum, one must consider the temperature and density differences between the equatorial and polar regions (see Eq. (11) of Badalyan 1986b and the small correction of Badalyan and Livshits 1992). If we assume that at the equator during solar minimum $n_0 = 2 \times 10^8$ cm^{-3} and $T = 1.4 \times 10^6$ K and at the poles $n_0 = 10^8$ cm^{-3} and $T = 10^6$ K, then for the emission measure at minimum we find that $EM = 10^{49}$ cm^{-3}. For the smallest values of n_0 and T given in Table 2 and Figures 4 and 5, i.e., $n_0 = 1.5 \times 10^8$ cm^{-3} and $T = 1.4 \times 10^6$ K at the equator and $n_0 = 0.6 \times 10^8$ cm^{-3} and $T = 0.95 \times 10^6$ K at the poles, we calculate $EM = 5 \times 10^{48}$ cm^{-3} from Badalyan (1986b). This would be the minimal value of the coronal emission measure.

Determining the emission measure in this way does not account for the loops of the inner corona. In those loops the temperature is 2×10^6 K and the density is 10^9 cm^{-3}. The coronal emission measure determined from X-ray observations is due to those structures and averages 10^{50} cm^{-3} at solar maximum. Therefore the coronal emission measure excluding the loops, obtained herein, is approximately half of the loop emission measure, or a third of the total emission measure.

These results also allow us to calculate the total coronal mass at maximum. The number of electrons in a spherically symmetric corona extending, for example, to $10R_\odot$ is given by

$$N = 4\pi \int_{R_\odot}^{10R_\odot} n(r)\, r^2\, dr. \tag{6}$$

For $n(r)$ we have used the distribution calculated by Badalyan (1988) assuming a Parker flow of plasma in an isothermal corona beginning at $2R_\odot$. Then, taking $n_0 = 4 \times 10^8$ cm^{-3}, we find that $N \approx 5 \times 10^{41}$ electrons. The number of positive charges is the same because of electrical neutrality. If helium abundance is 10%, then the average particle mass is about 2.2×10^{24} g, and the total coronal mass excluding loops is 1.1×10^{18} g. In the loop component with $EM = 10^{50}$ and average density of 10^9 cm^{-3} there are 10^{41} particles, so the entire mass of the corona is 1.3×10^{18} g.

For the typical solar wind flux of 2×10^8 cm^{-2} s^{-1} in the ecliptic at 1 AU, i.e., for a mass loss of 3.5×10^{19} g yr^{-1}, the corona must be replenished every two weeks.

8 COMMENTS ON THE METHOD OF ANALYSIS

We have shown, both in earlier papers (e.g., Badalyan and Livshits, 1985, 1986b; Badalyan, 1986a) and in this work, that numerous observational plots of ln B_K or ln pB versus $R_\odot/\rho$, especially those of great accuracy, strictly follow the theoretical curve calculated for hydrostatic density distribution in the middle corona from 1.2 to 2–2.5$R_\odot$.

Substantial differences are almost certainly due to experimental errors. For example, one can often see the same systematic error repeated at all position angles in an author's data. Another manifestation of experimental error are the differences among several authors in the brightness function at the same position angle in a given eclipse. An example of latter is found in Figure 3 for the eclipse of 12 November 1966: the data of Waldmeier (1967) in the east direction deviate above the theoretical curve, while those of Saito and Hata (1970) are below it, furthermore, the latter data show the same systematic deviation at all position angles. Thus, in our view, the comparison of the observations with the theoretical curve can indicate the accuracy of observations.

Confirmation of the hydrostatic density distribution in the middle corona allows us to test the validity of various models of the solar wind source. These models must give brightness values agreeing with observations of the middle corona. For example, Badalyan and Livshits (1986a) showed that the assumption of a strongly nonradial expansion of the large-scale solar wind flow (Kopp and Holzer, 1976) leads to a density and brightness profile contradicting the observations.

From the previous discussion we see that for each data set the determination of the density distribution $n(r)$ must be carefully done for any mathematical procedure to find the density. The advantage of our method over the classical method of Baumbach (1937) or its modifications (e.g., Saito *et al.*, 1977) is that it allows the entire brightness curve to be examined at once, thereby minimizing the influence of observational errors at various coronal heights. Unfortunately, the white light data remain the basic source of information about physical conditions in the middle and outer corona. The nature of these observations does not allow us to model the detailed inhomogeneities.

9 CONCLUSIONS

We have determined the temperature and density of the middle and outer corona and their variations through the solar cycle on the basis of white light eclipse observations. It was shown that the temperature in equatorial regions remains remarkably constant at 1.4×10^6 K, while in polar regions (coronal holes) it varies from

0.9×10^6 K at solar minimum to 1.4×10^6 K at maximum. The density n_0 clearly shows an increase toward the maximum phase of the solar cycle at the equator, but in the polar regions a dependence on the cycle is not obvious.

Thus we can say that the physical conditions in the middle corona (as well as the shape of the corona at these distances) are affected by solar activity. The growth of activity causes an increase in the density of equatorial regions, presumably through the presence of streamers, and apparently an increase of temperature in coronal holes. This is connected with the properties and variations of the heating in the large scale structures and with the general problem of energy balance in the corona. It is not yet clear whether the processes heating these structures vary through the solar cycle.

At sufficiently large heights in the corona, some evidence of the locally developing outflow of plasma should be present in the white light observations. The hydrodynamic expansion of the hot corona is an essential factor in the coronal energy balance and probably in maintaining the constant temperature in the middle corona. To solve these problems, we need coronal observations at large heights adequate for quantitative analysis.

We further note the results presented here could be used to interpret EUV and X-ray data, especially in the height range of $1.5–2R_\odot$.

Acknowledgements

The author expresses her extreme gratitude to Dr. S. Kahler for useful discussions. This work was supported by the Russian Foundation for Basic Research, grant N94–02–03381.

References

Allen, C. W. (1956) *Monthly Notices Roy. Astron. Soc.* **116**, 69.
Arnquist, W. N. and Menzel, D. H. (1970) *Solar Phys.* **11**, 82.
Badalyan, O. G. (1986a) *Astron. Astrophys.* **169**, 305.
Badalyan, O. G. (1986b) *Astron. Zh.* **63**, 762.
Badalyan, O. G. (1988) *Astron. Zh.* **65**, 403.
Badalyan, O. G. (1991) *Astron. Zh.* **68**, 602.
Badalyan, O. G. and Livshits, M. A. (1985) *Astron. Zh.* **62**, 132.
Badalyan, O. G. and Livshits, M. A. (1986a) *Solar Phys.* **103**, 385.
Badalyan, O. G. and Livshits, M. A. (1986b) *Astron. Zh.* **63**, 1029.
Badalyan, O. G. and Livshits, M. A. (1989) *Astron. Zh.* **66**, 832.
Badalyan, O. G. and Livshits, M. A. (1992) *Astron. Zh.* **69**, 377.
Badalyan, O. G., Livshits, M. A. and Sýkora, J. (1993) *Solar Phys.* **145**, 279.
Baumbach, S. (1937) *Astron. Nachr.* **263**, 121.
Cimino, M. and Croce, V. (1965) *Mem. Soc. Astron. Ital.* **36**, 3.
Dollfus, A. and Mouradian, Z. (1981) *Solar Phys.* **70**, 3.
Dürst, J. (1973) *Astron. Mitt. Zürich*, No. 320.
Dürst, J. (1974) *Astron. Mitt. Zürich*, No. 335.
Dürst, J. (1979) *Astron. Mitt. Zürich*, No. 372.
Dürst, J. (1982) *Astron. Astrophys.* **112**, 241.
Gillett, F. C., Stein, W. A. and Ney, E. P. (1964) *Astrophys. J.* **140**, 292.
Hata, S. and Tojo, A. (1972) *Ann. Tokyo Astron. Obs.* **13**, No. 2, 149.

Hepburn, N. (1955) *Astrophys, J.* **122**, 445.
Khetsuriani, Ts. S., Tetruashvili, E. I., Kiladze, R. I., *et al.* (1971) *Bull. Abastuman. Astrophys. Obs.*, No. 40, 55.
Khetsuriani, Ts. S., Salukvadze, G. N., Tetruashvili, E. I., *et al.* (1975) *Bull. Abastuman. Astrophys. Obs.*, No. 46, 163.
Kopp, R. A. and Holzer, T. E. (1976) *Solar Phys.* **49**, 43.
Koutchmy, S., Dzubenko, N. I., Nesmjanovich, A. T., and Vsekhsvjatsky, S. K. (1974) *Solar Phys.* **35**, 369.
Koutchmy, S. and Lamy, P. L. (1985) In *Properties and Interactions of Interplanetary Dust.*, R. H. Giese and P. Lamy (eds.), Dordrecht: Reidel Publ. Co., 63.
Koutchmy, S. and Magnant, F. (1973) *Astrophys. J.* **186**, 671.
Koutchmy, S. and Nitschelm, C. (1984) *Astron. Astrophys.* **138**, 161.
Leksa, I. (1963) *Bull. Astron. Inst. Czechosl.* **14**, 140.
Löchel, K. and Högner, W. (1965) *Zs. Astrophys.* **62**, 121.
Michard, R. and Sotirovsky, P. (1965) *Ann. Astrophys.* **28**, 96.
Mikhel'son, N. N. (1955) *Soobsch. Pulkovsk. obs.* **19**, No. 153, 57.
Nesmjanovich, A. T. (1958) In *Polnyje Solnechnyje Zatmenija 1952 i 1954 gg*, Ed. Acad. Sci. USSR, Moscow, 223.
Nesmjanovich, A. T., Dzubenko, N. I., and Khomenko, Yu. A. (1971a) *Astron. Tsirkular*, No. 606, 2.
Nesmjanovich, A. T. and Popov, O. S. (1976) *Soln. Dannye*, No. 4, 78.
Nesmjanovich, A. T., Popov, O. S. and Khomenko, Yu. A. (1971b) *Astron. Vestnik* **5**, No. 1, 42.
Newkirk, G. (1967) *Ann. Rev. Astron. Astrophys.* **5**, 213.
Nikolsky, G. M. (1954) *Astron. Zh.* **31**, 372.
Owaki, N. and Saito, K. (1967) *Publ. Astron. Soc. Japan.* **19**, No. 3, 279.
Rušin, V. and Rybanský, M. (1976) *Bull. Astron. Inst. Czechosl.* **26**, 160.
Rušin, V. and Rybanský, M. (1983) *Bull. Astron. Inst. Czechosl.* **34**, 265.
Saito, K. (1956) *Publ. Astron. Soc. Japan.* **8**, No. 3/4, 126.
Saito, K. (1970) *Ann. Tokyo Obs.* **12**, No. 2, 53.
Saito, K. (1972) *Ann. Tokyo Astron. Obs.* **13**, No. 2, 93.
Saito, K. and Hata, S. (1970) *Ann. Tokyo Astron. Obs.* **12**, No. 2, 151.
Saito, K., Poland, A. I., and Munro, R. H. (1977) *Solar Phys.* **55**, 121.
Saito, K. and Yamashita, Ya. (1962) *Ann. Tokyo Obs.* **7**, No. 4, 163.
Street, J. L. and Lacey, L.B. (1982) *Proc. Indian Nat. Sci. Acad.*, Part A, Suppl. No. 3, 81.
Van de Hulst, H. C. (1950) *Bull. Astron. Inst. Netherl.* **11**, 135.
Vitinsky, Yu. I., Kopecky, M., and Kuklin, G. V. (1986) *Statistika Pjatnoobrazovatelnoi Dejatelnosti Solntsa*, Moscow, Nauka.
Von Klüber, H. (1958) *Monthly Notices Roy Astron. Soc.* **118**, 201.
Vsekhsvyatsky, S. K., Dzyubenko, N. I., Ivanchuk, V. I., Popov, O. S., Rubo, G. A., Koutchmy, S., Koutchmy, O., and Stellmacher, G. (1981) *Astron. Zh.* **58**, 376.
Waldmeier, M. (1957) *Zs. Astrophys.* **43**, 289.
Waldmeier, M. (1959) *Zs. Astrophys.* **48**, 9.
Waldmeier, M. (1962) *Zs. Astrophys.* **55**, 187.
Waldmeier, M. (1963) *Zs. Astrophys.* **57**, 212.
Waldmeier, M. (1964) *Zs. Astrophys.* **60**, 28.
Waldmeier, M. (1966) *Zs. Astrophys.* **63**, 242.
Waldmeier, M. (1967) *Zs. Astrophys.* **67**, 463.
Waldmeier, M., Arber, H., and Bachman, H. (1957) *Zs. Astrophys.* **42**, 156.
Waldmeier, M. and Weber, S. E. (1969) *Astron. Mitt. Zürich*, No. 293.
Waldmeier, M. and Weber, S. E. (1974) *Astron. Mitt. Zürich*, No. 329.